Cell Reports

Supplementary Information

Predicting drug response in human prostate cancer from preclinical analysis of *in vivo* mouse models

Antonina Mitrofanova, Alvaro Aytes, Min Zou, Michael M. Shen, Cory Abate-Shen, and Andrea Califano

Figure S1, Related to Figure 1.

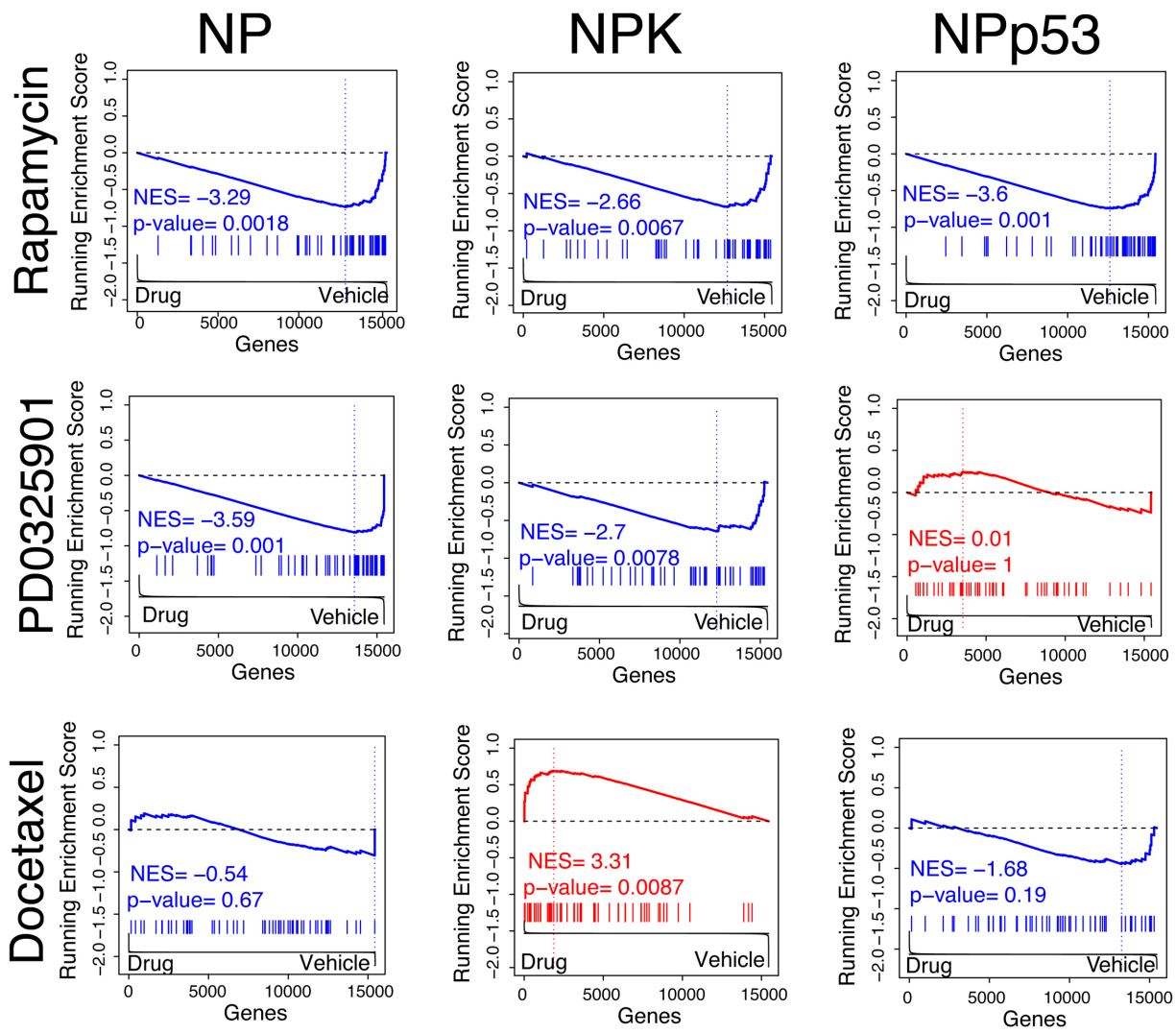

Legend: Examples of GSEA plots used to calculate the predicted global reversion score *(GRS)* as shown in Figure 1. The reference signatures represent the differential gene expression of three representative drugs, namely rapamycin, PD0325901, and docetaxel, versus vehicle, on three representative mouse models, namely *NP*, *NPK, and NPp53* mice, and human FOXM1/CENPF target genes as the query gene set.

Figure S2, Related to Figure 2

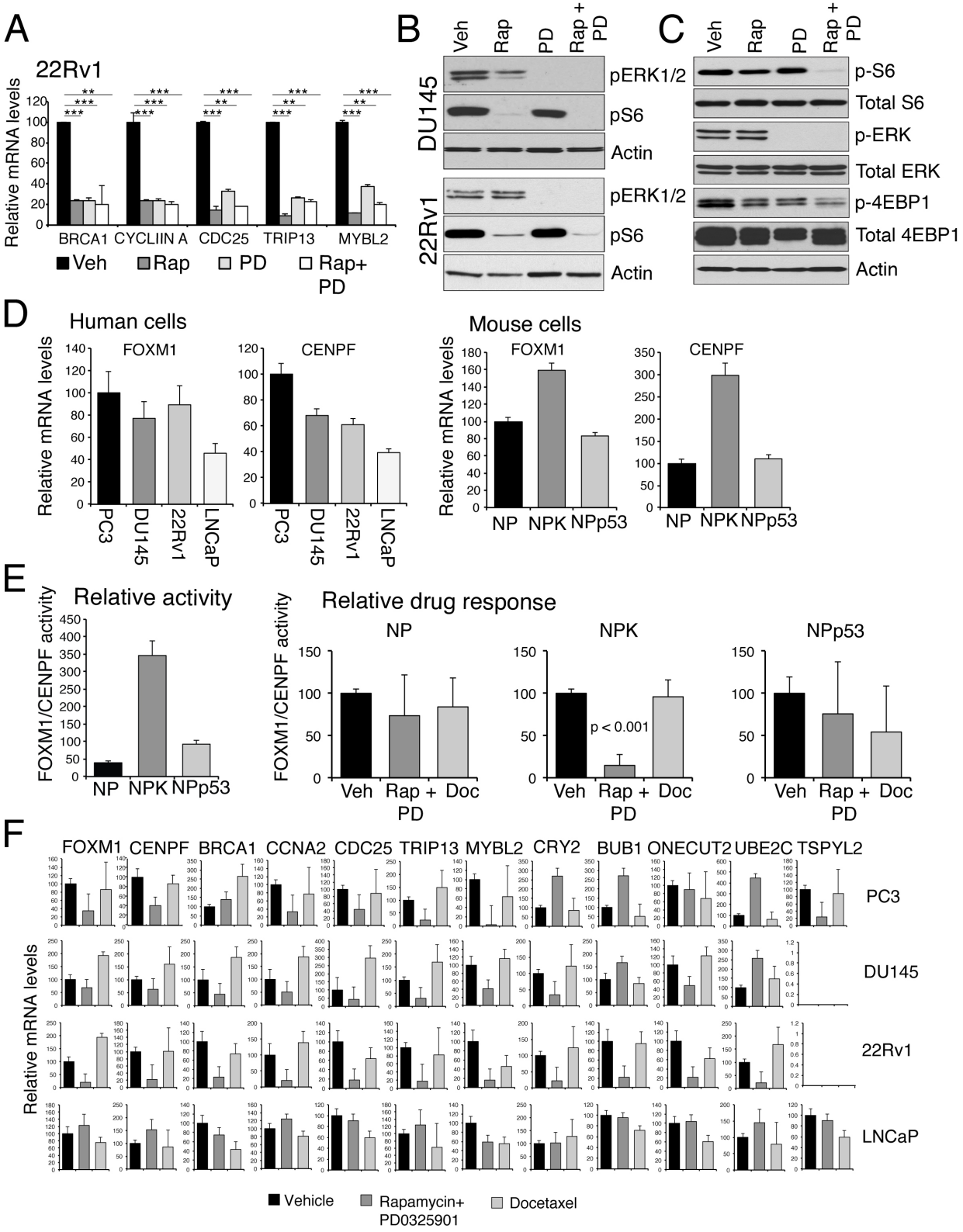

Legend: (A) Real-time PCR analyses showing the mRNA expression levels of *FOXM1* and *CENPF* and their shared target genes following treatment of 22Rv1 human prostate cancer cells with rapamycin and/or PD0325901 as indicated. (B, C) Western blots showing expression of markers of PI3-kinase/mTOR and MAP kinase signaling pathways following treatment with rapamycin and/or PD0325901, as indicated, in human DU145 or 22Rv1 prostate cancer cells (in panel B) and mouse *NPK* prostate cancer cells (in panel C). (D) mRNA expression levels of FOXM1 and CENPF in a panel of human (PC3, DU145, 22Rv1 and LNCaP) and mouse (NP, NPK and NPp53) prostate cancer cell lines. (E) (*Left)* Relative Activity of FOXM1/CENPF in the *NP*, *NPK* and *NPp53* mouse prostate cancer cells lines. Activity levels were calculated from expression levels of 10 independent FOXM1/CENPF target genes (see Detailed Experimental Procedures). *(Right)* Relative drug response of FOXM1/CENPF activity levels in mouse prostate cancer cell lines as assessed following treatment with rapamycin + PD0325901 (Rap+PD), or docetaxel (Doc), as indicated. (F) mRNA expression levels for FOXM1 and CENPF and the indicated targets following treatment with rapamycin + PD0325901 or docetaxel in the indicated human prostate cancer cell lines. Differences between treatment groups were assessed using Student's t-test, values are represented as mean ± standard deviation (SD).

Figure S3, Additional studies related to Figure 2

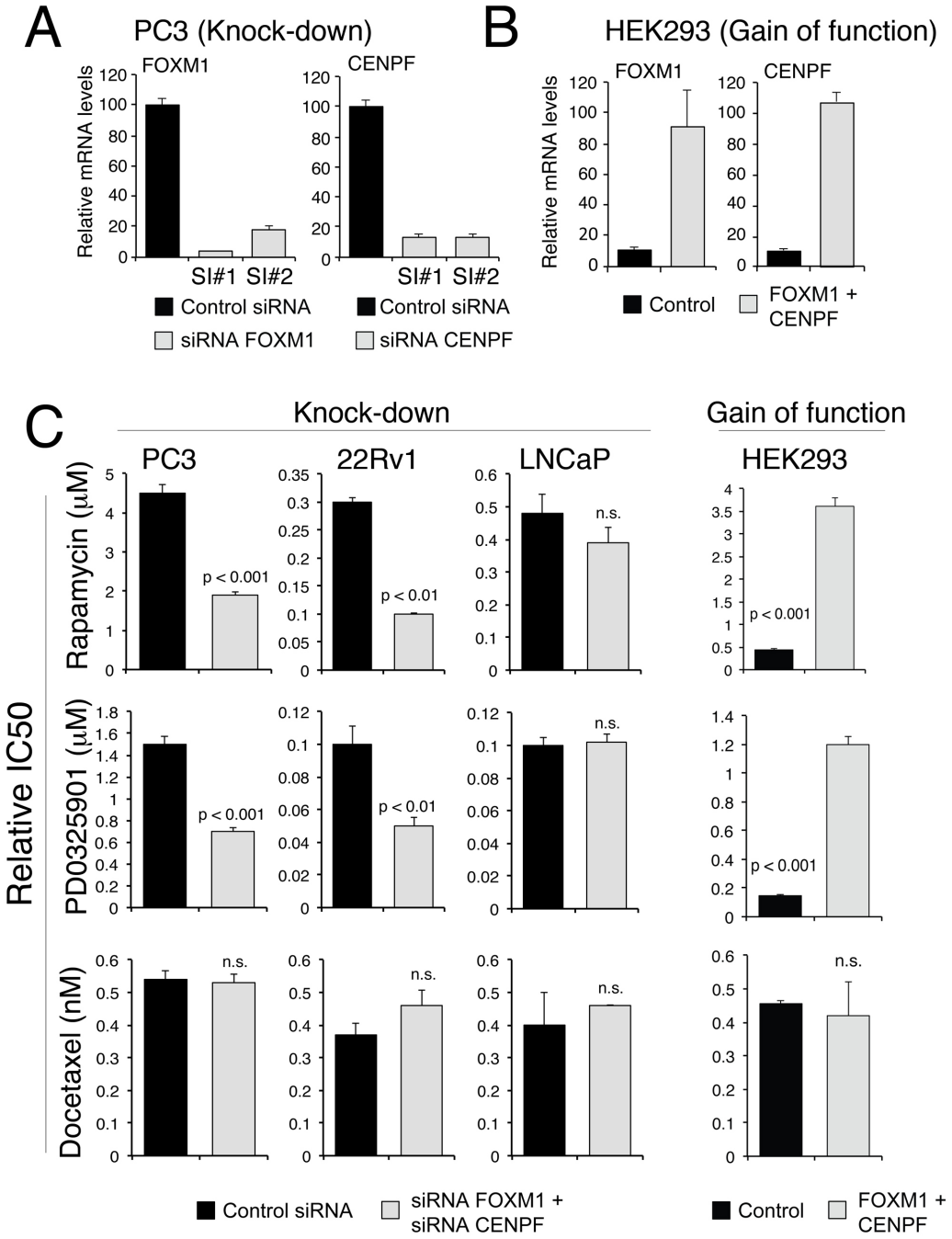

Legend: (A, B) Real time PCR showing the change of mRNA expression levels of FOXM1 or CENPF following their depletion (knock-down) using siRNA in PC3 prostate cancer cells (in panel A), or their forced expression (gain of function) in HEK293 cells. (C) Summary of the change in IC50 for rapamycin, PD0325901, or docetaxel treatment following knock-down of FOXM1/CENPF in PC3, 22Rv1 and LNCaP prostate cancer cells as indicated (*Left)*, or gain of function of FOXM1/CENPF in HEK293 cells (*Right*). Differences between treatment groups were assessed using Student's t-test; values are represented as mean ± standard deviation (SD).

Figure S4, Related to Figure 4

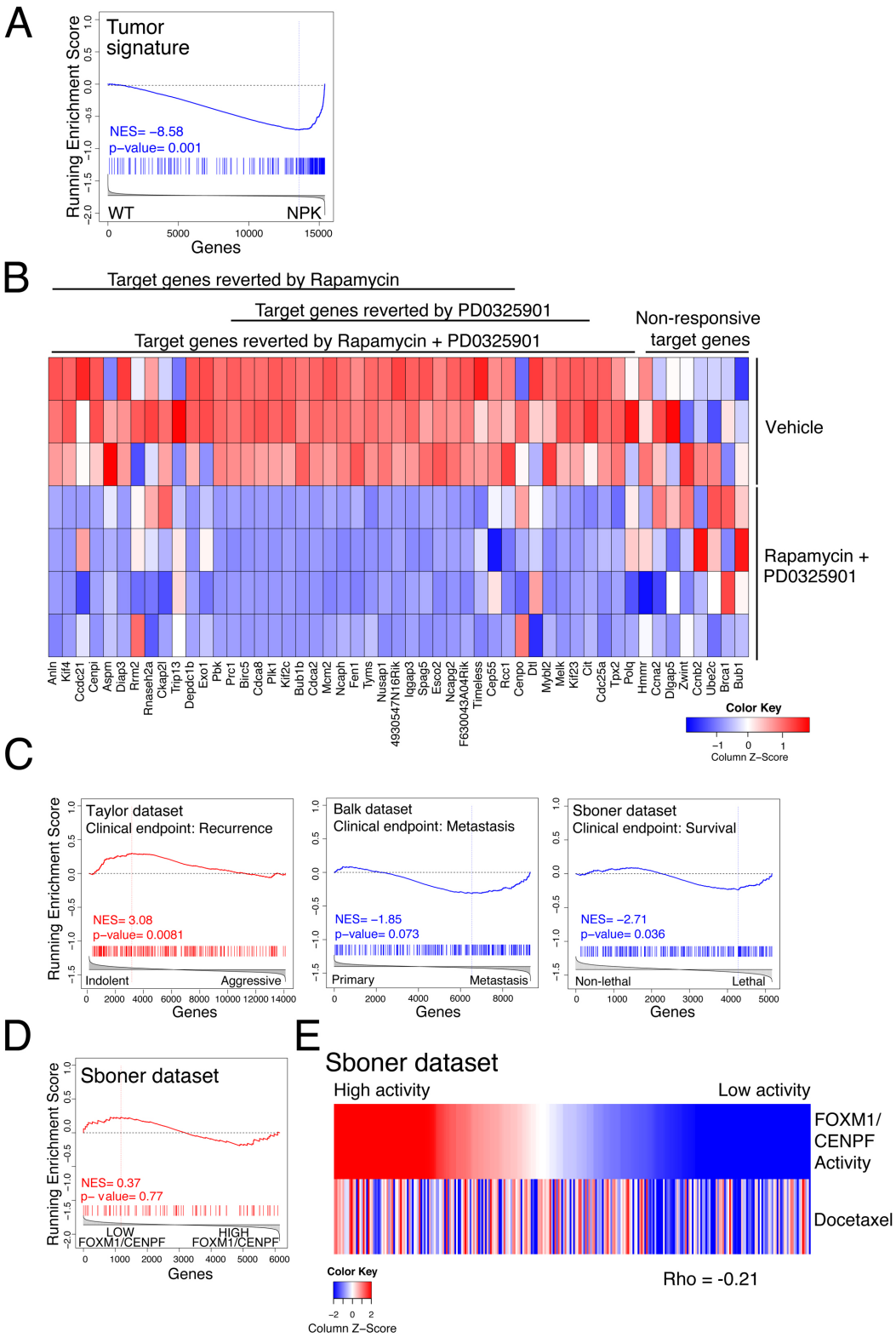

Legend: (A) GSEA using as the reference a mouse tumor signature that represents differentially expressed genes comparing phenotypically wild-type mouse prostate (WT) with *NPK* mouse tumors (see Aytes et al., 2014). The query gene set was the "therapeutic response" signature, which represents differentially expressed genes comparing *NPK* mouse tumors with vehicle versus rapamycin + PD0325901 for 1 month (see Fig. 3A and Table S3).
(B) Heat-map showing the relative expression levels of FOXM1/CENPF target genes after treatment of allografted tumors with vehicle versus rapamycin + PD0325901 (see Table S3). Shown are target genes affected by rapamycin and/or PD0325901, and genes that are non-responsive to these drugs.
(C) Comparison of three human prostate cancer signatures (*i.e.,* Taylor, Balk, and Sboner) as the reference and a humanized version of the mouse "docetaxel treatment" signature as the query gene set. Normalized enrichment score (NES) and associated p-values are indicated.
(D) GSEA comparing the "human FOXM1/CENPF" signature as the reference and the humanized mouse "docetaxel treatment" signature as the query gene set. The "human FOXM1/CENPF" signature compares patients in the Sboner dataset having low versus high FOXM1/CENPF activity levels.
(E) Heat-map showing the correlation between FOXM1/CENPF activity levels (top row) and predicted docetaxel treatment response (bottom row) in patients from the Sboner dataset. FOXM1/CENPF activity levels were estimated using single-sample MARINa (ss MARINa, see Detailed Experimental Procedures) on each human patient. Treatment response for each patient was estimated by comparing to a humanized version of the mouse "docetaxel treatment" signature using GSEA.

Table S1, Related to Figure 1.

Computational prediction of reversion of FOXM1/CENPF target genes following drug perturbation *in vivo*. *(provided separately)*

A. Human target genes of FOXM1/CENPF
B. Mouse target genes of Foxm1/Cenpf

Table S2, Related to Figure 1.

Computational prediction of drug synergy for reversion of human target genes of FOXM1/CENPF. *(provided separately)*

Table S3, Related to Figures 3 and 4: Description of mouse and human datasets used in this study

New mouse datasets introduced in this study

Dataset	Mouse models	N	Description	GEO/Ref
Therapeutic response	• NPK tumors, Vehicle • NPK tumors, Rap+PD	5 5	Expression profiles from NPK tumor-bearing mice treated for 1 month with rapamycin + PD0325901 or Vehicle.	Geo: GSE69211
Dynamic response (primary tumors)	• NPK tumors, Vehicle • NPK tumors, Rap+PD • NPK tumors, Docetaxel	5 5 5	Expression profiles from primary tumors treated with rapamycin + PD0325901, Docetaxel or Vehicle for 5 consecutive days.	
Dynamic response (allografted tumors)	• Allografted NPK tumors, Vehicle • Allografted NPK tumors, Rap+PD	3 4	Expression profiles from allografted tumors grown in *nude* mice, treated with Rapamycin +PD0325901 or Vehicle for 5 consecutive days.	Geo: GSE69213

Mouse dataset reported previously

Signature	Mouse models	N	Description	GEO/Ref
Drug perturbation signature	• Wild-type • Myc • NP • NPp53 • NPB • NPK	28 28 28 28 28 28	Expression profiles from drug-perturbed mice treated for 5 days with each of 13 perturbagens (or Vehicle).	Geo: GSE53202 Ref: (Aytes et al., 2014)

Human signatures/datasets

Signature	Description	N	Geo/Ref
Taylor malignancy signature	• Gleason 6 with no biochemical recurrence • Gleason ≥ 8 with biochemical recurrence by 3 years	39 10	Geo: GSE21034 Ref (dataset): (Taylor et al., 2010) Ref (signature): (Aytes et al., 2013)
Balk metastasis signature	• Hormone naïve prostate tumors • Bone metastases from castration-resistant prostate cancer	22 29	Geo: GSE32269 Ref (dataset): (Stanbrough et al., 2006) Ref (signature): (Aytes et al., 2014)
Sboner survival signature	• Transurethral specimens from patients that survived following prostate cancer diagnosis for at least 16 years. • Transurethral specimens from patients who died of prostate cancer within 12 months	12 6	Geo: GSE16560 Ref (dataset): (Sboner et al., 2010) Ref (signature): (Wang et al., 2013)

Table S4, Related to Figure 4.

Pathway analysis comparing drug treatment of *NPK* mice with Rapamycin +PD0325901 versus vehicle for the dynamic response primary tumor cohort (see Table S3). (*provided separately)*

Table S5, Related to Figures 2-5 and Experimental Procedures

Oligonucleotides sequences used in this study

Gene name	Sequence	
	Forward	**Reverse**
Human		
FOXM1	CGTCGGCCACTGATTCTCAAA	GGCAGGGGATCTCTTAGGTTC
CENPF	CTCTCCCGTCAACAGCGTTC	GTTGTGCATATTCTTGGCTTGC
BRCA1	GCTCGTGGAAGATTTCGGTGT	TCATCAATCACGGACGTATCATC
CCNA2	CGCTGGCGGTACTGAAGTC	GAGGAACGGTGACATGCTCAT
CDC25	ACGCACCTATCCCTGTCTC	CTGGAAGCGTCTGATGGCAA
TRIP13	ACTGTTGCACTTCACATTTTCC	TCGAGGAGATGGGATTTGACT
MYBL2	CCGGAGCAGAGGGATAGCA	CAGTGCGGTTAGGGAAGTGG
WHSC1	GCCAAACTGCGTTTTGAGTCC	TGTTCCTTCTCGCCTTGTTTTC
ASF1B	TCATCCGAGTGGGCTACTACG	GTTGTTGTCCCAGTTGATATGGA
TOP2A	TTAATGCTGCGGACAACAAACA	CGACCACCTGTCACTTTCTTTT
UHRF1	AGGTGGTCATGCTCAACTACA	CACGTTGGCGTAGAGTTCCC
SUV39H1	CATCTGGGACGCATCACTGTA	TCACCAACACGGTACTCATTG
BLM	GGACCTTGACACCTCTGACAG	GGATTCAGCTCCTGCATACTCA
E2F1	ACGTGACGTGTCAGGACCT	GATCGGGCCTTGTTTGCTCTT
MCM2	ATGATCGAGAGCATCGAGAACC	GCCAAGTCCTCATAGTTCACCA
MCM4	CACCACACACAGTTATCCTGTT	CGAATAGGCACAGCTCGATAGAT
UBEC2	GACCTGAGGTATAAGCTCTCGC	TTACCCTGGGTGTCCACGTT
BUB1	AGCCCAGACAGTAACAGACTC	GTTGGCAACCTTATGTGTTTCAC
CRY2	TCCCAAGGCTGTTCAAGGAAT	TGCATCCCGTTCTTTCCCAAA
TSPYL2	GCTTCTGGGTCAAAGCATTC	CCTGCAGATTGGTCAAGTAGC
HNF4G	TTGCAGGTTCAGTCGGCAAT	TTTCATTCCCGCTCTAAAACACT
E2F7	TAGCTCGCTATCCAAGTTATCCC	CAATGTCATAGATGCGTCTCCTT
ONECUT2	AACGCAAAGAGCAAGAACCAA	AAGATGGCGAAGAGTGTTCGG
ZNF165	ACCAAGGCCCATTTTGATTCA	CTCTGAGACTCCCCTGATTCTT
ACTIN	GTCTGCCTTGGTAGTGGATAATG	TCGAGGACGCCCTATCATGG
GAPDH	TGTGGGCATCAATGGATTTGG	ACACCATGTATTCCGGGTCAAT
Mouse		
Foxm1	CAGAATGCCCCGAGTGAAACA	GTGGGGTGGTTGATAATCTTGAT
Cenpf	ACATTGCGAGACATCAGGCTT	TTGGGGTATTTTCCTGTTGCC
Brca1	CGAATCTGAGTCCCCTAAAGAGC	AAGCAACTTGACCTTGGGGTA
CcnA2	AAGAGAATGTCAACCCCGAAAAA	ACCCGTCGAGTCTTGAGCTT
Cdc25	GGCAAACCTAAGCATTCTGTCG	CCAGAGGTCCAGATGAATCCA
Trip13	AGCCTCGTGTATGATGTGGAG	ACCCGGTTCCAGGTGATGA
Mybl2	CTGGCACAACCACCTCAAC	CAGCGGTTACCCAGGACTTT
Whsc1	TGCCAAAAAGGAGTACGTGTG	CTTCGGGAAAGTCCAAGGCAG
Asf1b	CAACTGGGACAACAATCCAGAC	CCTGGGATGCAACTAGGGAG
Top2a	CAACTGGAACATATACTGCTCCG	GGGTCCCTTTGTTTGTTATCAGC
Uhrf1	CTCAGCACCCTTAAAGGAGAGG	CAATCGGTGACGGACCGTTAG

Suv39h1	CTGTGCCGACTAGCCAAGC	ATACCCACGCCACTTAACCAG
Blm	AGCGACACTCAGCCAGAAAAC	GCCTCAGACACGTTCACATCTT
E2f1	GAGAAGTCACGCTATGAAACCTC	CCCAGTTCAGGTCAACGACAC
Mcm2	ATCAGAACTACCAACGTATCCGC	GTCAGCTCTATCTCGTCCCC
Mcm4	ATCCACAACCGATCATTCTTCTC	GGACAATAGTGTGAGGTGTCTG
Ube2c	CTCCGCCTTCCCTGAGTCA	GGTGCGTTGTAAGGGTAGCC
Bub1	AGAATGCTCTGTCAGCTCATCT	TGTCTTCACTAACCCACTGCT
Cry2	GCGTCTGTTTGTAGTCCGGG	TCCCAAAGGGTTCAGAGTCATA
Tspyl2	TGCCCTATGTCATTCTTGAGGA	GGAGCGTTTCCATGATCCCT
Hnf4g	TACCACAGACAACGGTGTCAA	AAGAAACCCTTGCACCCATCA
E2f7	GCATACGGCCAGATCCGAG	GACCCTTGTCTTTCTCCCTGT
Onecut2	ACACCACGCCATGAGTATGTC	GCGTCAGCGTAGTGTAGGT
Znf165	AGCCACGATGGATGTGAGAG	GCTGCATGTTTAGCAAGTTTTGG
Actin	GGCTGTATTCCCCTCCATCG	CCAGTTGGTAACAATGCCATGT
Gapdh	CTAGAGAGCTGACAGTGGGTAT	AGACGACCAATGCGTCCAAA
siRNA oligonucleotides		
Target	**Sense (5' -> 3')**	**Antisense (5' -> 3')**
siFOXM1#1	GGAUCAAGAUUAUUAACCAtt	UGGUUAAUAAUCUUGAUCCca
siFOXM1#2	CACUAUCAACAAUAGCCUAtt	UAGGCUAUUGUUGAUAGUGca
siCENPF#1	GCUACAACUUUUAUCCGAAtt	UUCGGAUAAAAGUUGUAGCtc
siCENPF#2	CCUCAUGAGUUGUCAACAAtt	UUGUUGACAACUCAUGAGGcc

Detailed Experimental Procedures

Analyses of drug perturbation *in vivo*

Transcriptional target genes of FOXM1/CENPF were predicted from the mouse or human prostate cancer interactomes, as described in (Aytes et al., 2014). This study focused on shared target genes of FOXM1/CENPF, which are primarily activated (rather than repressed). *In vivo* drug perturbation of a series of GEM models each treated with 13 different pertubagens (or vehicles) was described previously (Aytes et al., 2014). This information is summarized below.

Description of drug perturbagens		
Perturbagen	**Target(s)**	**Description**
Steroid hormone signaling		
Testosterone	Androgen receptor	Steroid hormone that is converted to dihydrotestosterone for binding to the androgen receptor
Calcitriol	Vitamin D receptor	Biologically active form of vitamin D3; binds to vitamin D receptor
Enzalutamide	Androgen receptor	Inhibits androgen receptor by preventing nuclear translocation
Signaling pathways		
MK2206	Akt	Allosteric inhibitor of Akt1, Akt2 and Akt3 phosphorylation
LY294002	PI3-kinase	Inhibits binding of ATP binding to the catalytic subunit of PI3-kinase
Rapamycin	mTOR	Selectively binds mTORC1 thus blocking signaling that leads to p70S6 kinase activation.
PD0325901	MEK1/2	Competitive inhibitor of MEK1/2 that binds the ATP binding domain preventing phosphorylation
Kinase inhibitors		
Imatininb	Bcr-Abl, c-kit, PDGFR	Inhibits binding to ATP binding domain and thereby inhibits tyrosine kinase activity
Dasatinib	Src, Bcr-Abl	Small molecule inhibitor of SRC and BCR/ABL tyrosine kinases through binding to the ATP binding domain
Sorafenib	ERK,VEGF, PDGFR, FGFR, Braf	Inhibits extracellular receptor tyrosine kinases and intracellular kinases through binding to the ATP binding domain
Other		
BAY 11-7082	IkBα; NFkβ	Inhibits phosphorylation of IκBα
WP1066	JAK/STAT, ERK1/2	Inhibits phosphorylation of JAK2, STAT3, STAT5, and ERK1/2
Docetaxel	Tubulin	Inhibits microtubule assembly (standard chemotherapy)

Description of GEM models				
Abbrev.	**Genotype**	**Description**	**Prostate phenotype**	**Reference**
WT	*N/A*	Wild-type control	Normal	NA
NP	*Nkx3.1$^{CreERT2/+}$; Pten$^{flox/flox}$*	Inducible deletion of *Pten*	HG-PIN/ Adenocarcinoma	(Floc'h et al., 2012)
NPp53	*Nkx3.1$^{CreERT2/+}$; Pten$^{flox/flox}$; p53$^{flox/flox}$*	Inducible deletion of *Pten* plus *p53*	HG-PIN/ Adenocarcinoma	Floc'h and Abate-Shen (unpublished)
Myc	*ARR$_2$PB-Myc (Hi-Myc)*	Transgene expressing c-Myc	HG-PIN/ Adenocarcinoma	(Ellwood-Yen et al., 2003)
NPB	*Nkx3.1^{CreERT2}; Pten$^{flox/flox}$; Braf$^{LSL-V600E/+}$*	Inducible deletion of *Pten* plus inducible activation of *Braf$^{V600E/+}$*	Adenocarcinoma with metastasis (30% of cases)	(Wang et al., 2012)
NPK	*Nkx3.1$^{CreERT2/+}$; Pten$^{flox/flox}$; Kras$^{LSL-G12D/+}$*	Inducible deletion of *Pten* plus inducible activation of *Kras$^{G12D/+}$*	Adenocarcinoma with metastasis (100% of cases)	(Aytes et al., 2013)

Drug perturbation signatures were defined by differential gene expression between drug- and vehicle-treated mice using either t-test (for samples ≥3) or fold change (for samples ≤ 2). Since the shared targets of FOXM1/CENPF that are the focus of these study are activated and not repressed, reversion was estimated using one-tail gene set enrichment analysis (GSEA). However, in principle, these analyses can be done using two-tailed gene set GSEA to estimate the reversion of either activated or repressed target genes. The significance of enrichment was defined by normalized enrichment score (NES, which we refer to as Reversion score or RS_{MR}) and *p*-value, estimated with gene shuffling (for samples ≤ 5) or sample shuffling (for samples ≥ 6). Global reversion scores (*GRS*) were defined by integration of NESs for a given drug j across all GEM models, in which it was tested, using a metric based on the Stouffer integration formulation (Whitlock, 2005) defined as:

$\mathrm{GRS(j)} = \sum_{i=1}^{N} \mathrm{NES(j},i)/\sqrt{\mathrm{N}}$ where N is a total number of mouse models in which drug j was administered, and $NES(\mathrm{j},\mathrm{i})$ is a Normalized Enrichment Score estimated for drug j in mouse model i. A summary of the *GRS* for each drug is provided in Table S1.

Pairwise-analysis was done with each possible combination to estimate whether a given drug pair inhibits more target genes compared to each drug individually. In particular, assuming that, in mouse model i, drug j inhibits $x(j,i)$ number of targets, drug k inhibits $y(k,i)$ number of targets, the number of common targets inhibited by both drug j and drug k is $q(j,k,i)$, and the number of total targets affected by both drugs inhibit is $t(j,k,i) = x(j,i) + y(k,i) - q(j,k,i)$. The number of targets inhibited uniquely by drug j (when compared to drug k) is defined as

$$x^u(\mathrm{j},\mathrm{i}) = x(j,i) - q(j,k,i)$$

and the number of targets uniquely inhibited by drug k (when compared to drug j) is defined as

$$y^u(\mathrm{k},\mathrm{i}) = y(k,i) - q(j,k,i)$$

We then estimated the synergistic reversion score (*SRS*) for drug j and drug k in model i through the F1 statistical measure (harmonic mean), which combines x^u and y^u, which would be maximized only if both x^u and y^u are maximized,

$$SRS'(\mathrm{j},\mathrm{k},\mathrm{i}) = \frac{2 * x^u(j,i) * y^u(k,i)}{x^u(j,i) + y^u(k,i)}$$

The *SRS'* was further normalized by the total number of targets affected by both drugs in mouse model i, using F1-score (harmonic mean) so that both variables are maximized:

$$SRS(\mathrm{j},\mathrm{k},\mathrm{i}) = \frac{2 * \mathrm{SRS}'(\mathrm{j},\mathrm{k},\mathrm{i}) * \mathrm{t}(j,k,i)}{SRS'(j,k,i) + \mathrm{t}(j,k,i)}$$

These calculations were applied for each pair of drugs and for each mouse model and the global synergy reversion score (*GSRS)* for each pair of drugs (j,k) across all mouse models was estimated as an average *SRS* weighted by the number of models in which drug j and drug k show non-zero SRS, such as

$$\mathrm{GSRS}(\mathrm{j},\mathrm{k}) = -\frac{L}{N}\sum_{i=1}^{N} SRS(j,k,i)$$

where N is a total number of mouse models in which drugs j and k were administered, $x^u(j,i)$ is a number of targets uniquely inhibited by drug j in model i, $y^u(k,i)$ is a number of targets uniquely inhibited by drug k in model i, $t(j,k,i)$ is a number of total targets inhibited by drugs j and k in model i, and L is a number of mouse models for which drug j and drug k have positive $x^u(j,i)$ and $y^u(k,i)$ (i.e., drug j and drug k show some level of affecting different transcriptional targets). The pairwise global synergistic reversion scores are provided in Table S2.

To estimate the statistical significance of the *GSRS* for a given drug pair, we compared the calculated score to a random model, in which we selected a random set of genes of the same size as the FOXM1/CENPF regulon. This random gene set was then used as a query gene set for each drug pair of interest to estimate a *GSRS* for the random model. This process was repeated 1000 times and a p-value was estimated by comparing *GSRS* from the actual data analysis to the random model (*i.e.*, the number of times the GSRS from the random model is greater or equal to the GSRS from the actual data).

Analyses of drug treatment in culture

Rapamycin and docetaxel were purchased from LC labs (Catalog #R-5000 and #D1000, respectively); PD0325901 was a generous gift from Pfizer (Batch U). Cell culture studies were done using human prostate cancer cell lines, PC3, DU145, 22Rv1, and LNCaP, and human embryonic HEK293 cells, obtained from ATCC. Parallel studies were performed using cell lines derived from GEM models (see previous section), including a cell line from the *NPK* mouse model, which was previously described (Aytes et al., 2013) and two new cell lines from the *NP* and *NPp53* mouse models, which will be described in a subsequent publication (*in preparation*). Exponentially growing cells were treated with rapamycin (3 μM), PD0325901 (1 μM) or docetaxel (1 nM) for 24 hours. *In vitro* studies were done as described previously (Aytes et al., 2013; Wang et al., 2012). Colony formation was visualized by staining with crystal violet and quantified using ImageJ software (NIH; http://imagej.nih.gov/ij/). A t-test was used to calculate the significance (*p*-value) of the difference between drug- and vehicle-treated cells using assays performed at least two times, each done in triplicate.

Real-time qPCR was performed using the Quantitech SYBR Green PCR kit (Qiagen) and relative levels of mRNA expression data were calculated using the comparative CT Method (ΔΔCT Method) as we have done previously (Aytes et al., 2014). To calculate the relative activity of FOXM1/CENPF, real time PCR was done on each target gene in each cell line and for

each drug treatment; the relative activity was inferred by averaging the expression levels of the target genes using the following formula:

$$Activity\ (\mathrm{FOXM1/CENPF}) = \sum_{w=1}^{R} \frac{\mathrm{Exp\ (w)}}{R}$$

where Exp(w) is the expression levels of target gene w, and R is the total number of tested targets w for transcriptional regulator of interest. Comparison of differences among the groups was carried out by two-tailed Student's *t*-test. Oligonucleotides used for real-time PCR are described in Table S5.

For determination of IC50, HEK293 cells were co-transfected with pLX304-FOXM1-V5 (CCSB ORFeome collection) and pUHD30F-CENPF-FLAG (kind donation from Dr. Xue Liang Zhu, Shanghai Institutes for Biological Sciences) mammalian expression vectors and treated with rapamycin (0.3 mM to 0.03 nM) + PD0325901 (0.1 mM to 0.01 nM) or docetaxel (0.1 μM to 0.01 pM) for 72 hours. Alternatively, PC3, 22Rv1 and LNCaP cells were transfected with siRNA oligonucleotides (see Table S5) to co-silence FOXM1 and CENPF and treated with rapamycin + PD0325901 or docetaxel as above. Cell viability was determined using the Vybrant® MTT Cell Proliferation Assay Kit (Invitrogen, Carlsbad, CA). All cell culture assays were performed a minimum of two independent experiments each done in triplicate; data are represented as mean ± SD. A t-test was used to calculate the significance (*p*-value) of the difference in IC50 between drug- and vehicle-treated cells. GraphPad Prism software (Version 5.0) was used for determining IC50 and for statistical analysis.

Analyses of drug treatment *in vivo*

NPK mice were induced to form tumors by delivery of tamoxifen as in (Aytes et al., 2013); drug treatment was initiated at 1-2 months following tumor induction. Allografted tumors were established from *NPK* prostate tumors (~3 months after tumor induction) by implantation of a ~2^3 mm^3 piece of freshly dissected tumor into the subcutaneous space of the flank of male athymic mice (NCr/Nude, Taconic). Drug treatment was initiated when allografted tumors reached a volume of ~10^3 mm^3, typically 2-3 weeks after implantation.

Mice were treated with vehicle or rapamycin via intraperitoneal delivery (10 mg/kg in 5.3% Tween-80, 5.2% of PEG-400) and/or PD0325901 via oral gavage (10 mg/kg in 0.05% hydroxy-propyl-methylcellulose, 0.02% Tween-80); docetaxel was delivered intraperitoneally (10 mg/kg in 23% Tween 80 in PBS). For therapeutic response or survival cohorts (see Fig. 3A), mice were treated for 5 consecutive days with 2 days off for a period of four weeks, as in (Kinkade et al., 2008), with subsequent sacrifice for tumor collection or further monitoring for survival. For the dynamic response cohort, mice were treated for 5 consecutive days (in the morning) and the tumors were collected on the 5^{th} day (in the afternoon).

MRI imaging was done before and after drug treatments using a 200 MHz Bruker 4.7T Biospec scanner equipped with a 400 mT/m ID 12 cm gradient (Bruker Biospin MRI GmbH, Ettlingen, Germany) as in (Aytes et al., 2013). At the time of sacrifice, a full necropsy was performed and prostate (or other) tissues were collected for analysis by hematoxylin and eosin (H&E) staining, immunohistochemical staining, and quantitation of Ki67-expressing proliferating cells were done as in (Aytes et al., 2013; Kinkade et al., 2008). Analysis of disseminated tumor cells (DTCs) from bone marrow was done using PCR as described (Aytes et al., 2013). As above, RNA expression levels were analyzed by real-time qPCR using the Quantitech SYBR Green PCR kit (Qiagen) (Aytes et al., 2014). Statistical analyses were performed using a two-tailed t-test, or Log-rank test (for survival). GraphPad Prism software (Version 5.0) was used for all statistical analysis and to generate data plots.

Cross-species computational analysis of drug treatments signatures

Gene expression profiles were generated from primary or allografted tumors from vehicle- or drug-treated mice (as in Table S3) using the mouseWG-6 v2 BeadArrays (Illumina) as described in (Aytes et al., 2014). Drug signatures were defined by differential gene expression between vehicle- and drug-treated tumors using t-test statistics. For comparison with human gene signatures as well as pathway analyses, the mouse genes were mapped to their corresponding human orthologs based on the homoloGene database (NCBI), which defined "humanized" mouse signatures used herein. Pathway enrichment analysis was performed by GSEA using the "humanized" dynamic drug response signatures (see Table S3) as a reference. The query gene set were pathways collected from the C2 database, which includes pathways from REACTOME (Croft et al., 2011), KEGG (Ogata et al., 1999), and BioCarta (http://www.biocarta.com/genes/allpathways.asp). A summary of biological pathways that are altered following drug treatment is provided in Table S4.

To evaluate the conservation of gene expression changes following drug treatment of mouse tumors relative to human cancer, the "humanized" dynamic response mouse signatures were compared with human gene signatures from the Taylor (GSE21034) (Taylor et al., 2010), Balk (GSE32269) (Stanbrough et al., 2006), and Sboner (GSE16560) (Sboner et al., 2010) datasets. The human gene signatures are summarized in Table S3, and were described previously, (Aytes et al., 2013; Aytes et al., 2014; Wang et al., 2013).

The relationship of gene expression changes following drug treatment of mouse tumors with FOXM1/CENPF activity levels in human patients was evaluated using the Sboner dataset (GSE16560) (Sboner et al., 2010). First, FOXM1/CENPF activity levels in each human sample in the Sboner dataset were estimated using single sample MARINa (ssMARINa) as in (Aytes et al., 2014) based on expression of their transcriptional targets inferred from the human prostate cancer interactome. For this analysis, the Sboner dataset was scaled so that each sample was compared to the average of all samples (Aytes et al., 2014). Next, using the estimated FOXM1/CENPF activity levels, a "FOXM1/CENPF activity" signature was defined by differential gene expression between human samples with low FOXM1/CENPF activity levels (negative NES, $p < 0.01$) and human samples with high FOXM1/CENPF activity levels (positive NES, $p < 0.01$) using t-test statistics. This "FOXM1/CENPF activity" signature was then compared to the "humanized" dynamic treatment response mouse signatures using GSEA.

To evaluate the correlation between FOXM1/CENPF activity levels in the human patients and the mouse drug treatment response, drug response was estimated with GSEA using each human sample in the Sboner dataset queried with downregulated genes (using the top 200 genes) in the humanized "dynamic response" signature. Correlation of the human FOXM1/CENPF activity levels in the Sboner dataset and the mouse dynamic treatment response was estimated using Spearman correlation coefficient.

Treatment-responsive genes were identified using the standard MAster Regulator INference algorithm (MARINa) (Lefebvre et al., 2010) by interrogating the mouse prostate cancer interactome (Aytes et al., 2014) with the rapamycin + PD0325901 dynamic drug response signature. For comparison with human prostate cancer, the mouse genes were "humanized", as above, and their expression levels and genomic alterations in the Taylor human prostate cancer dataset (Taylor et al., 2010) were assessed using cBioportal (Cerami et al., 2012; Gao et al., 2013). For comparison of the activity levels of the treatment-response genes in human patients, the Sboner dataset was used to infer "ssMARINa", as above. The activity levels for the humanized treatment-response genes were used to calculate the COX proportional

hazard model, Kaplan-Meier analysis, and association with drug response. COX proportional hazard model and Kaplan-Meier analysis were done using the “surv” and “coxph” functions from the survcomp package in R v2.14.0; the COX *p*-value was calculated using the Wald test. For Kaplan-Meier survival analysis, *k-means* clustering was done on the activity levels of the treatment-response genes to cluster patients into two groups: one group having increased overall activity of the treatment-response genes and one group having decreased overall activity**.** The predictive power of the treatment-response genes was compared to that of a comparable group of transcriptional regulators selected at random; analysis was repeated 1000 times, so that p-value reflected the number of times an equally sized random set of transcriptional regulators performed at least as well or better compared to the original set of treatment-responsive genes.

Additional References

Cerami, E., Gao, J., Dogrusoz, U., Gross, B. E., Sumer, S. O., Aksoy, B. A., Jacobsen, A., Byrne, C. J., Heuer, M. L., Larsson, E.*, et al.* (2012). The cBio cancer genomics portal: an open platform for exploring multidimensional cancer genomics data. Cancer discovery *2*, 401-404.

Croft, D., O'Kelly, G., Wu, G., Haw, R., Gillespie, M., Matthews, L., Caudy, M., Garapati, P., Gopinath, G., Jassal, B.*, et al.* (2011). Reactome: a database of reactions, pathways and biological processes. Nucleic Acids Res *39*, D691-697.

Ellwood-Yen, K., Graeber, T. G., Wongvipat, J., Iruela-Arispe, M. L., Zhang, J., Matusik, R., Thomas, G. V., and Sawyers, C. L. (2003). Myc-driven murine prostate cancer shares molecular features with human prostate tumors. Cancer Cell *4*, 223-238.

Floc'h, N., Kinkade, C. W., Kobayashi, T., Aytes, A., Lefebvre, C., Mitrofanova, A., Cardiff, R. D., Califano, A., Shen, M. M., and Abate-Shen, C. (2012). Dual targeting of the Akt/mTOR signaling pathway inhibits castration-resistant prostate cancer in a genetically engineered mouse model. Cancer research *72*, 4483-4493.

Gao, J., Aksoy, B. A., Dogrusoz, U., Dresdner, G., Gross, B., Sumer, S. O., Sun, Y., Jacobsen, A., Sinha, R., Larsson, E.*, et al.* (2013). Integrative analysis of complex cancer genomics and clinical profiles using the cBioPortal. Science signaling *6*, pl1.

Ogata, H., Goto, S., Sato, K., Fujibuchi, W., Bono, H., and Kanehisa, M. (1999). KEGG: Kyoto Encyclopedia of Genes and Genomes. Nucleic Acids Res *27*, 29-34.

Wang, J., Kobayashi, T., Floc'h, N., Kinkade, C. W., Aytes, A., Dankort, D., Lefebvre, C., Mitrofanova, A., Cardiff, R. D., McMahon, M.*, et al.* (2012). B-Raf activation cooperates with PTEN loss to drive c-Myc expression in advanced prostate cancer. Cancer research *72*, 4765-4776.